Applied Mathematical Modelling 36 (2012) 2935–2946

Contents lists available at SciVerse ScienceDirect

Applied Mathematical Modelling

journal homepage: www.elsevier.com/locate/apm

Heat and mass transfer investigation of rotating hydrocarbons droplet which behaves as a hard sphere

J. Dgheim [a,*], M. Abdallah [a], R. Habchi [a], N. Zakhia [b]

[a] Lebanese University Faculty of Sciences II, Fanar, Beirut, P.O. Box 90656, Jdeideh, Lebanon
[b] University of The Holy Spirit – Kaslik, Faculty of Engineering, P.O. Box 446, Jounieh, Lebanon

ARTICLE INFO

Article history:
Received 6 April 2011
Received in revised form 19 September 2011
Accepted 21 September 2011
Available online 2 October 2011

Keywords:
Rotating sphere
Transfer numbers
Correlation
Droplet evaporation
Hydrocarbons

ABSTRACT

The steady state boundary layer equations around rotating pure hydrocarbon droplet are solved numerically. The droplet is simulated to behave as a hard sphere. The transfer equations are discretized using an implicit finite difference method where Thomas algorithm solves the system of algebraic equations. Moreover, dimensionless parameters of heat and mass transfer phenomena around a rotating hexane droplet concluded. The thickness of the boundary layer is unknown for this model and therefore, it is determined. Further, this work proposes correlations of Nusselt and Sherwood numbers for monocomponent hydrocarbon droplets in evaporation. These correlations consider the rotation phenomena and further, the variation of the thermophysical and transport properties in the vapour phase.

1. Introduction

Research in liquid droplet in evaporation and combustion systems has been for a long time the subject of many engineering applications such as engines and turbo machines. Numerical studies of droplet evaporation phenomenon have progressed in the last twenty years with the development of numerical techniques and experimental tools. The first approach consists of studying the behaviour of an isolated droplet in evaporation. For instance, Chauveau et al. [1], Deplanque and Sirignano [2] showed numerical and empirical correlations of Nusselt and Sherwood numbers for droplets in evaporation phenomena. Chauveau et al. used a camera of infrared thermography and a thermocouple to measure the mean and the surface temperature of opaque hydrocarbon droplet in evaporation and, as a result, they proposed empirical correlations for heat and mass transfer numbers. Deplanque and Sirignano solved Navier–Stokes equations using a finite difference method and proposed numerical correlations of Nusselt and Sherwood numbers. Bouaziz et al. [3] used the same techniques for hydrocarbon droplet in evaporation in natural and forced convection.

Heat and mass transfers analyses in natural convection of pure isolated droplet in evaporation are reported by Gebhart and Hieber [4], Yuge [5] and Amato and Tien [6] and thus correlations expressing Nusselt number in function of Grashof or Rayleigh numbers are determined. Moreover, Ranz and Marshall [7] have proposed semi-empirical correlations for the evaporation of hydrocarbon droplet in natural and forced convections. These correlations express Nusselt and Sherwood numbers as a function of Grashof or Reynolds, Prandtl and Schmidt numbers. Chen and Mucoglu [8] solved numerically the mixed convection equations and studied the heat transfer around a sphere. Renksizbulut and Yuen [9] studied numerically and experimentally the heat and mass transfers around a sphere in saturated single fuel in evaporated forced convection flow.

* Corresponding author. Tel.: +961 3 16 20 77; fax: +961 1 68 15 53.
E-mail address: jdgheim@ul.edu.lb (J. Dgheim).

0307-904X/$ - see front matter © 2011 Elsevier Inc. All rights reserved.
doi:10.1016/j.apm.2011.09.078

Nomenclature

B	spalding transfer number
C	concentration
CG	known nondimensional variables
Cp	specific heat (J kg^{-1} K^{-1})
d	sphere diameter (m)
D	diffusion coefficient (m^2 s^{-1})
L	latent heat (J kg^{-1})
M	molar mass (kg kmol^{-1})
Nu	Nusselt number
P	pressure (atm)
Pr	Prandtl number
r	sphere radius (m)
Re_m	rotator Reynolds number
Sh	Sherwood number
Sc	Schmidt number
T	temperature (K)
u	velocity component in x direction (m s^{-1})
v	velocity component in y direction (m s^{-1})
w	velocity component in z direction (m s^{-1})
Y	mass fraction

Greek letters

β	expansion number
Δ	difference
ε	error
λ	thermal conductivity (W m^{-1} K^{-1})
μ	dynamic viscosity (kg m^{-1} s^{-1})
ν	kinematic viscosity (m^2 s^{-1})
ρ	density (kg m^{-3})
θ	polar angle (°)
ω	spinning velocity (rps)

Subscripts

a	air
$crit$	critical
ebn	ebullition
f	fuel
I	incrementation step in x direction
J	incrementation step in y direction
g	gas
l	liquid
max	maximum
M	mass
s	surface
sat	saturated
T	thermal
∞	ambient medium

Superscripts

$*$	dimensionless values
$-$	mean

The major of the determined correlations consider a sphere saturated with a pure liquid in evaporation or in combustion without taking into account the effect of the transfers around a rotating droplet [10].

Sazhin [11] considered heat and mass transfer correlations of fuel droplets analyzing the convective and the radiative heating modes of nonevaporating droplets. He reported the classical models of the droplets evaporation phenomena and developed Nusselt and Sherwood semi-empirical correlations.

The rotating sphere is a crucial phenomenon in systems such as internal combustion engines where the droplet is injected into the combustion chamber in a rotational motion. Therefore, this phenomenon remains vital pertaining to evaporation and combustion studies.

Numerical studies concerning rotating droplet in evaporation phenomenon have been considered little compared to those for an isolated stagnant droplet in forced and natural convections. For example, Kreith et al. [12] have proposed, in boundary layer laminar regime, an empirical correlation for a rotating sphere in an infinite medium:

$$\overline{Nu} = 0.43 Re_m^{0.5} Pr^{0.4} \quad \text{where} \quad Re_m = d^2\omega/v_\infty Re_m < 5 \times 10^4. \tag{1}$$

The above equations consider uniform thickness in the vicinity of a rotating sphere.

Saikrishnan and Roy [13,14] studied the influence of temperature dependency, viscosity and Prandtl number on the steady laminar forced convection flow over a rotating sphere using boundary layer equations solved by finite difference scheme. Garrett and Peake [15] analysed the convective and the instabilities in the boundary layer flow over the outer surface of a rotating sphere in still fluid. Their results show that a crossflow instability mode is most risky when it is below 66°.

Poon et al. [16] simulate three different flow regimes for a stationary sphere, from steady axisymmetric, and steady to unsteady planar-symmetric and deduced that the state of the wake structures depends strongly on the rotation axis angle.

2. Mathematical model

The boundary layer equations are carried out numerically for a sphere of radius, r_s, rotating around its vertical axis at a constant spinning velocity, ω, saturated with a pure liquid hydrocarbon and placed in a semi-infinite medium. The ambient pressure is supposed to be equal to 1 atmosphere and the ambient temperature, T_∞, varies between 300 K and 1000 K. This model assumes laminar and steady flow around the rotating sphere and neglect surface tension, chemical reaction, radiation, Soret and Dufour effects.

Therefore, the heat and mass transfer equations around a rotating sphere are written in 2-D Cartesian coordinates where (Fig. 1) x is the curvilinear coordinate and y is positive towards outside the rotating sphere.

Boundary conditions:

a. At the droplet surface ($y = 0$):

$$\begin{aligned} u &= 0 \\ v &= \frac{D_M}{Y_s - 1}\frac{\partial Y}{\partial y}\Big|_S, \\ w &= r_s\omega\sin\theta, \\ T &= T_s, \\ Y &= Y_s. \end{aligned} \tag{2}$$

b. Far from the droplet ($y \to \infty$):

$$\begin{aligned} u &= 0, \\ w &= 0, \\ T &= T_\infty, \\ Y &= Y_\infty, \end{aligned}$$

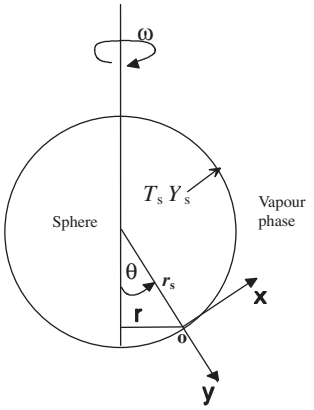

Fig. 1. Resolution around a droplet assimilated to a sphere.

Introducing the dimensionless variables:

$$x^* = \frac{x}{r_s}, \quad r^* = \frac{r}{r_s}, \quad T^* = \frac{T - T_\infty}{T_s - T_\infty}, \quad Y^* = \frac{Y - Y_\infty}{Y_s - Y_\infty}, \quad \rho^* = \frac{\rho}{\rho_\infty}, \quad \lambda^* = \frac{\lambda}{\lambda_\infty},$$

$$\mu^* = \frac{\mu}{\mu_\infty}, \quad Cp^* = \frac{Cp}{Cp_\infty}, \quad D_M^* = \frac{D_M}{D_\infty}, \quad u^* = \frac{u}{r_s\omega}, \quad v^* = \frac{v}{r_s\omega}Re_m^{0.5}, \quad L^* = \frac{L}{L_v}, \tag{3}$$

$$w^* = \frac{w}{r_s\omega}, \quad Re_m = r_s^2\frac{\omega}{\nu_\infty}, \quad y^* = \frac{y}{r_s}Re_m^{0.5}, \quad \nu^* = \frac{\nu}{\nu_\infty}, \quad P^* = \frac{P}{P_\infty}, \quad Sc = \frac{\nu_\infty}{D_\infty}, \quad Pr = \frac{\nu_\infty}{\lambda_\infty}.$$

The equations of heat and mass transfer become:

Continuity equation

$$\frac{\partial}{\partial x^*}(\rho^* u^* r^*) + \frac{\partial}{\partial y^*}(\rho^* v^* r^*) = 0. \tag{4}$$

Momentum equation

$$\rho^* u^* \frac{\partial u^*}{\partial x^*} + \rho^* v^* \frac{\partial u^*}{\partial y^*} - \rho^* \frac{w^{*2}}{r^*}\frac{dr^*}{dx^*} = \frac{\partial}{\partial y^*}\left(\mu^* \frac{\partial u^*}{\partial y^*}\right), \tag{5}$$

$$\rho^* u^* \frac{\partial w^*}{\partial x^*} + \rho^* v^* \frac{\partial w^*}{\partial y^*} + \rho^* u^* \frac{w^*}{r^*}\frac{dr^*}{dx^*} = \frac{\partial}{\partial y^*}\left(\mu^* \frac{\partial w^*}{\partial y^*}\right). \tag{6}$$

Energy equation

$$\rho^* u^* \frac{\partial T^*}{\partial x^*} + \rho^* v^* \frac{\partial T^*}{\partial y^*} = \frac{1}{Cp^* Pr_\infty}\frac{\partial}{\partial y^*}\left(\lambda^* \frac{\partial T^*}{\partial y^*}\right) + \frac{\partial Y^*}{\partial y^*}\frac{\rho^*(D_{f,M}^* Cp_f^* - D_{a,M}^* Cp_a^*)(Y_s - Y_\infty)}{Cp^* Sc_\infty}\frac{\partial T^*}{\partial y^*}. \tag{7}$$

Diffusion equation

$$\rho^* u^* \frac{\partial Y^*}{\partial x^*} + \rho^* v^* \frac{\partial Y^*}{\partial y^*} = \frac{1}{Sc_\infty}\frac{\partial}{\partial y^*}\left(\rho^* D_M^* \frac{\partial Y^*}{\partial y^*}\right). \tag{8}$$

The dimensionless boundary conditions become:

Boundary conditions

a. At the droplet surface ($y^* = 0$):

$$\begin{aligned} &u^* = 0, \\ &v^* = \frac{D_M^*(Y_s - Y_\infty)}{Sc_\infty(Y_s - 1)}\frac{\partial Y^*}{\partial y^*}\bigg|_s, \\ &w^* = \sin\theta, \\ &T^* = 1, \\ &Y_s^* = 1, \end{aligned} \tag{9}$$

b. Far from the droplet ($y^* \to \infty$):

$$\begin{aligned} &u^* = 0, \\ &w^* = 0, \\ &T^* = 0, \\ &Y^* = 0, \end{aligned}$$

The mass fraction at liquid–vapour interface is a function of saturated vapour pressure which varies according to liquid surface temperature as reported by Dgheim [17]:

$$Y_s = \frac{P_{sat}M}{P_{sat}M + (P_\infty - P_{sat})M_a}, \tag{10}$$

where $P_\infty = 1$ atm and $P_{sat} = 133.32 \times e^{(15.83 - 2697.55/(T - 48.78))}$ is the saturated vapour pressure for hexane hydrocarbon droplet [17].

The latent heat of vaporization is a function of surface temperature variation, given by:

$$L = L_v((T_{crit} - T_s)/(T_{crit} - T_{ebn}))^{0.38}, \tag{11}$$

where L_v represents the fuel latent heat of vaporization [17].

Table 1
The dimensionless equation parameters.

f	c_f	a_f	b_f	d_f
u^*	0	1	μ^*	$\rho^* \frac{w^{*2}}{r^*} \frac{dr^*}{dx^*}$
w^*	0	1	μ^*	$-\rho^* u^* \frac{w^*}{r^*} \frac{dr^*}{dx^*}$
T^*	c_T	$1/Cp^* Pr_\infty$	λ^*	0
Y^*	0	$1/Sc_\infty$	$\rho^* D_M^*$	0

The local Nusselt and Sherwood numbers are defined as:

$$Nu_s = -x^* Re_m^{0.5} \left(\frac{\partial T^*}{\partial y^*}\right)_s \quad \text{and} \quad Sh_s = -Re_m^{0.5} \left(\frac{\partial Y^*}{\partial y^*}\right)_s, \tag{12}$$

The mean Nusselt and Sherwood numbers are:

$$\overline{Nu} = \frac{1}{2} \int_{\theta=0}^{\theta=180} Nu_s \sin\theta d\theta \quad \text{and} \quad \overline{Sh} = \frac{1}{2} \int_{\theta=0}^{\theta=180} Sh_s \sin\theta d\theta, \tag{13}$$

The vapour phase transfer equations are solved by taking into account the thermophysical and transport properties variability.

The density, viscosity, thermal conductivity, heat capacity, binary diffusion coefficient of the air–fuel vapour mixture and the latent heat of vaporization are computed using Lieberam [18], and Abramzon and Sirignano [19] correlations. These correlations show that the thermophysical properties are dependent on the temperature and compositions of the vapour phase. This analysis computes the thermophysical and transport properties at each node according to the local temperature T_g and the local fuel mass fraction Y_g in the vapour phase, as:

$$\overline{T}_g = \frac{(T_g + T_s)}{2} \quad \overline{Y}_g = \frac{(Y_g + Y_s)}{2}. \tag{14}$$

3. Numerical procedures

The Eqs. (4)–(8) and the boundary conditions (9) are solved by an implicit finite difference method. The stability study of the program leads to a dimensionless angle step of 0.36 and a space step of 2.10^{-3}. These values lead to a scheme of 181×1501. Prandtl number, Schmidt number and the spinning velocity are varied to keep the flow laminar.

The dimensionless Eqs. (4)–(8) can be rewritten in general form:

$$\rho^* u^* \frac{\partial f}{\partial x^*} + (\rho^* v^* - c_f) \frac{\partial f}{\partial y^*} = d_f + a_f \frac{\partial}{\partial y^*} \left(b_f \frac{\partial f}{\partial y^*}\right). \tag{15}$$

Table 1 yields to an equation system written as:

$$BG_J f_{J-1}^{l+1} + DG_J f_J^{l+1} + AG_J f_{J+1}^{l+1} = CG_J^l, \tag{16}$$

where (BG_J), (DG_J) and (AG_J) are the tridiagonal matrix coefficients.

This system has been solved by using Thomas algorithm (see Appendix A).

4. Results and discussion

Computations have been performed for various types of hydrocarbon fuels of molar mass varying between 86 and 142 g/mol and, particularly, for hexane liquid droplet, the more volatile liquid. The spinning velocity was chosen to be 5, 50, and 100 rps.

4.1. Results validation and new correlation for Sherwood number

The new correlation of Nusselt number is compared with Kreith model [10]. Fig. 2 shows the evolution of $(\overline{Nu} Pr^{-0.4})$ versus Reynolds number for various types of pure fuels (hexane, heptane, octane and decane). Further, this figure shows good agreement of this model with that of Kreith. The maximum relative error is 3.6% with $(0.7 < Pr < 0.86)$ and $(1 \leq Re_m \leq 10^5)$.

This analysis also considers the liquid phase evaporation effect to develop a new correlation of mass transfer coefficient $(\overline{Sh})$ in function of Schmidt (Sc) and Reynolds numbers for a rotating sphere.

The least square method is used to develop a new correlation for Sherwood number similar to that of Nusselt. The new correlation is made for hexane, heptane, octane and decane (Fig. 3) as:

$$\overline{Sh} = 0.43 Sc^{0.4} Re_m^{0.5} \quad \text{with} \quad 1.58 < Sc < 3.13, \varepsilon_{max} = 4\%), \quad 1 \leq Re_m \leq 10^5), \tag{17}$$

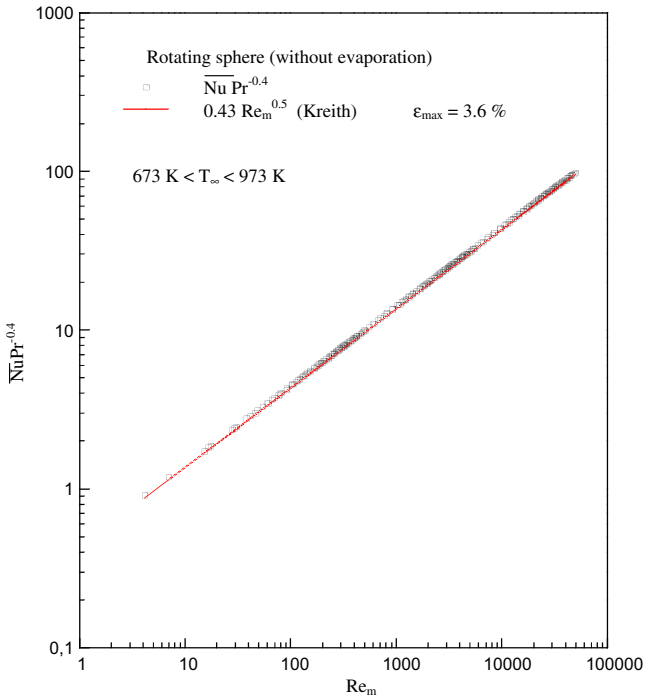

Fig. 2. Comparison between Kreith correlation and our correlation for a sphere of monocomponent hydrocarbons.

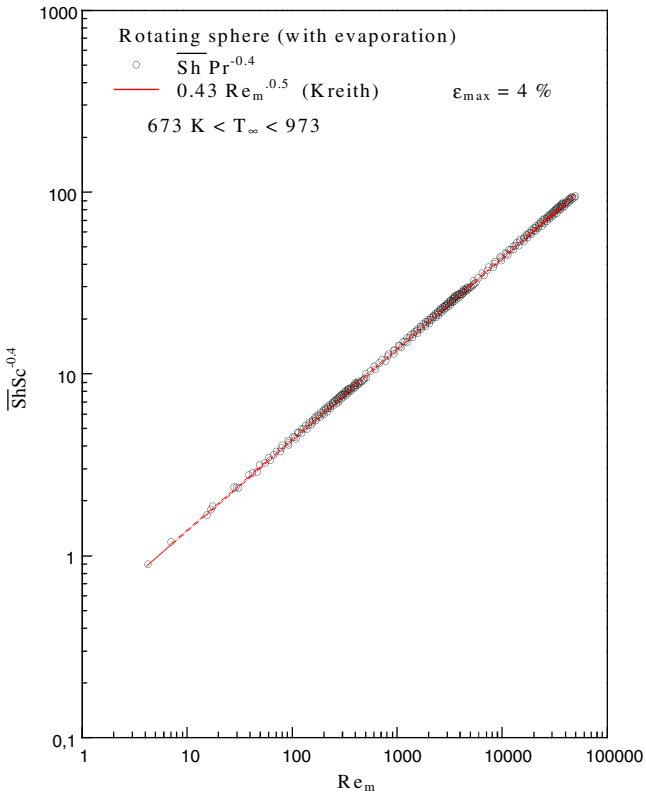

Fig. 3. Mean Sherwood number correlation for monocomponent hydrocarbons droplet.

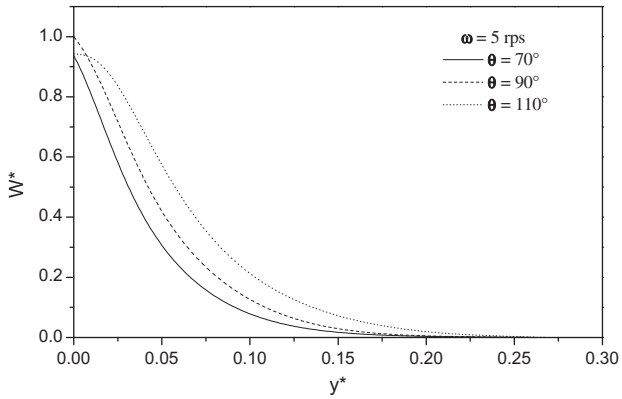

Fig. 4. Transversal velocity component evolution of hexane liquid droplet versus radial axis for various angles θ. Spinning velocity $\omega = 5$ rps.

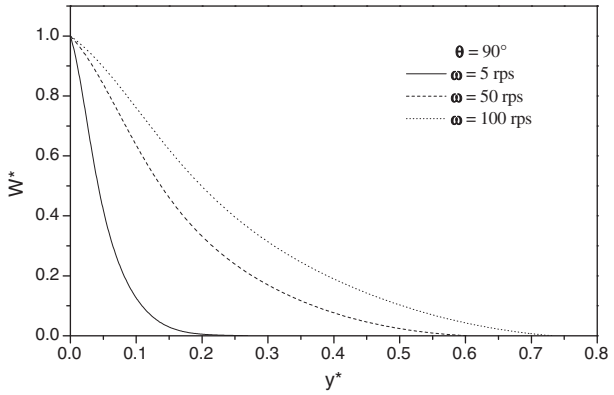

Fig. 5. Transversal velocity component evolution of hexane liquid droplet versus radial axis for various spinning velocities ω and at an angle $\theta = 90°$.

4.2. Physical parameters evolution

The z-component velocity in function of the radial direction for various angles is shown in Fig. 4 for hexane with spinning velocity of 5 rps. This figure shows that the initial value of the z-component velocity, varying from $\theta = 0°$ to $\theta = 90°$ (maximum increase) and back to zero at $\theta = 180°$, depends on the rotation angle and the spinning velocity, ω. Moreover, this velocity component decreases simultaneously from its initial value to zero far from the droplet surface and further, the vapour phase thickness, y^*, is an increasing function of the angle, θ. Thus, beyond an angle $\theta = 90°$, the evaporation of liquid hydrocarbon droplet develops buoyancy forces which create a thermal plume around the top of the liquid droplet. Furthermore, the vapour phase thickness, pushed by the repulsion forces, becomes significant, when approaching from the top of the droplet. Also, Fig. 5 indicates that this component changes in radial direction for different spinning velocities (ω).

The increasing of the spinning velocity, ω, increases the vapour phase thickness due to the increasing of the temperature gradient between the vapour phase and the ambient medium.

The spinning velocity of the liquid droplet also influences the temperature and the mass fraction of hexane droplet vapour phase. The temperature and the mass fraction decrease as a function of the radial direction as illustrated in Figs. 6–9 respectively.

These figures indicate a strong influence of the rotating droplet on physical parameters and boundary layer thickness. When the spinning velocity increases, the hydrocarbon droplet liquid phase evaporates very quickly and the released vapour is carried out by the movement of the vapour phase created from the spinning velocity of the droplet. Thus, the evolution of the boundary layer thickness is observed at an angle of 90°. In addition, increasing the spinning velocity, the heat and mass transfers of the vapour phase also increase and play a major role on the increasing vapour phase temperature and mass fraction gradients between the droplet surface and the ambient medium. Otherwise, these gradients would be higher for angles higher than 90°. This phenomenon is due to a thermal and mass plumes generated from the buoyancy forces.

At the bottom of the liquid droplet, the hot vapour is carried up quickly by the upwind generated from the buoyancy forces and moved away by the growth of the boundary layer thickness. The released vapour will be concentrated at the top of the liquid droplet forming a thermal plume (Fig. 10).

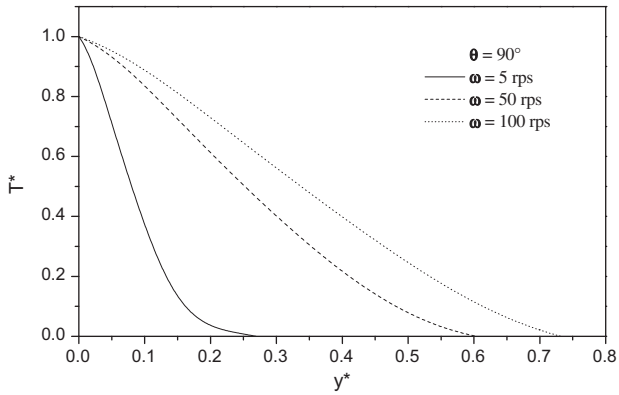

Fig. 6. Temperature evolution of hexane liquid droplet versus radial axis for various spinning velocities ω and at an angle $\theta = 90°$.

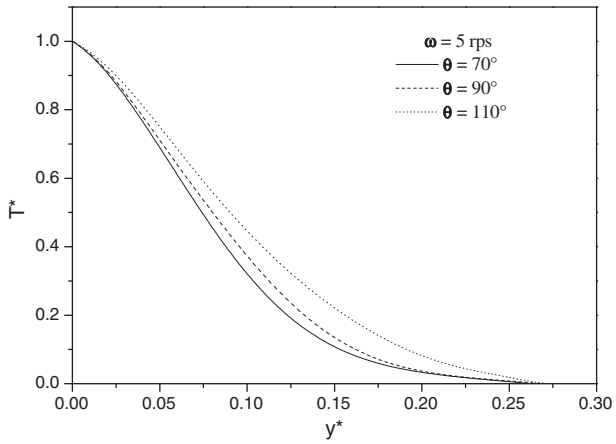

Fig. 7. Temperature evolution of hexane liquid droplet versus radial axis for various angles θ. Spinning velocity $\omega = 5$ rps.

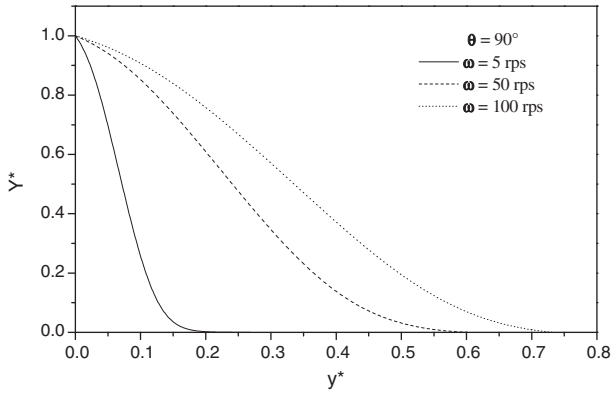

Fig. 8. Mass fraction evolution of hexane liquid droplet versus radial axis for various spinning velocities ω and at an angle $\theta = 90°$.

Fig. 11 shows the change of the radial velocity for various spinning velocities at an angle 90°. For higher spinning velocity, the flow moves away the released vapour towards a location where the rotation is weak. This results in increasing of the boundary layer thickness and decreasing of the radial velocity. For lower spinning velocity, the radial velocity becomes significant and close to the droplet surface. The parabolic profile is generated by the buoyancy forces whereas the double waves are due to the repulsion forces of the hexane rotating droplet.

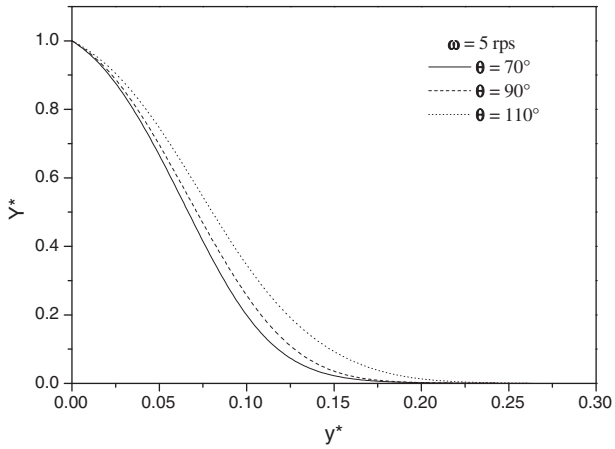

Fig. 9. Mass fraction evolution of hexane liquid droplet versus radial axis for various angles θ. Spinning velocity $\omega = 5$ rps.

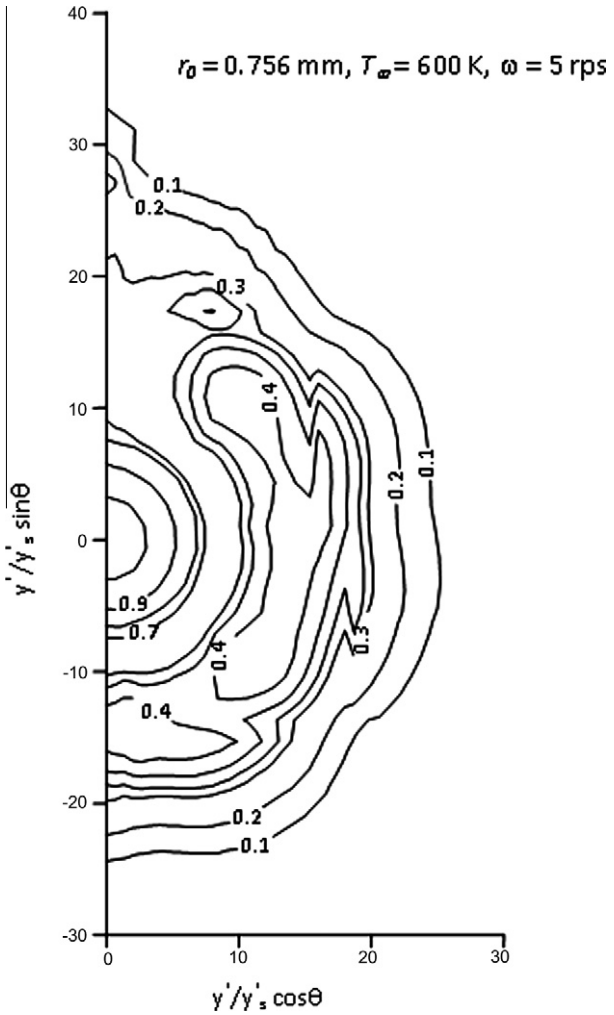

Fig. 10. Hexane vapour phase isotherms.

Furthermore, the radial velocity profile is too thin as well as close to the liquid droplet surface. When approaching from the top of the liquid droplet, the flow is entirely rightward and thus moves away from the droplet surface towards the region

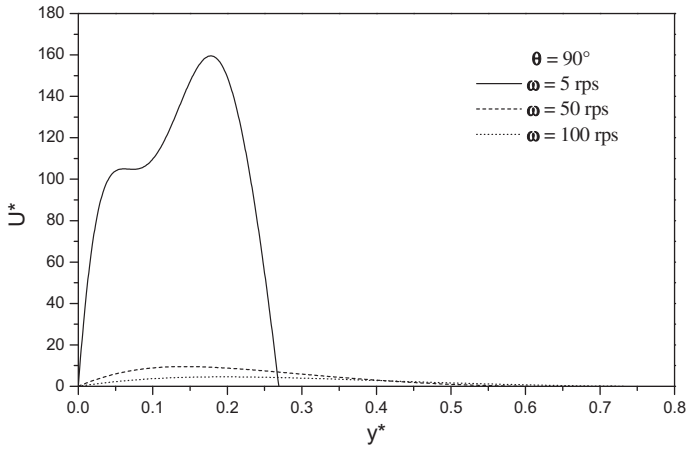

Fig. 11. Radial velocity evolution of hexane liquid droplet versus radial axis for various spinning velocities ω and at an angle $\theta = 90°$.

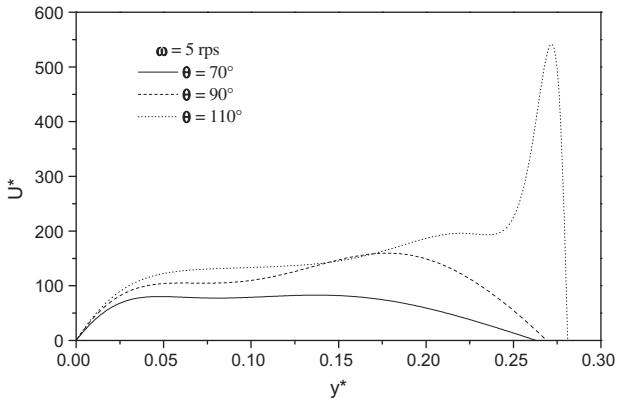

Fig. 12. Radial velocity evolution of hexane liquid droplet versus radial axis for various angles θ. Spinning velocity $\omega = 5$ rps.

of weak rotation. This phenomenon is due to both forces whose resultant pushes the first wave to be absorbed by the second one in a distance far from the liquid vapour interface (Fig. 12).

4.3. New correlations for rotating hydrocarbon droplet

Common correlations for different pure hydrocarbons are found and determined by least square method where the effect of Reynolds (Re_m), mass (B_M) and heat transfer (B_T) numbers is considered. They are:

$$\overline{Nu} = 1.13(1 + B_T)^{-2} Pr^{0.4} Re_m^{0.5} \quad 1 < Re_m < 5x10^4 \quad 0.7 < Pr < 0.86, \tag{18}$$

$$\overline{Sh} = 0.12(1 + B_M)^{-2.8} Sc^{0.4} Re_m^{0.5} \quad 1 < Re_m < 5.10^4 \quad 1.58 < Sc < 3.13, \tag{19}$$

where

$B_M = (Y_s - Y_\infty)/(1 - Y_s)$ and $B_T = Cp(T_s - T_\infty)/L$ are thermal and mass transfer numbers.

Fig. 13 shows the profiles of these correlations. The maximum error between the fitting function and the numerical outputs is less than 10%.

For low values of thermal and mass transfer numbers (B_T and $B_M << 1$) and $10 \leq Re_m \leq 5.10^4$, the average Nusselt and Sherwood numbers do not change significatively. For higher values of these numbers, Nusselt and Sherwood numbers decrease significatively due to higher rotation angle of the droplet. However, average Nusselt and Sherwood numbers increase with increasing Reynolds, Prandtl and Schmidt numbers, due to the fact that the heat and mass transfer decrease with the fuel volatility of the liquid droplet.

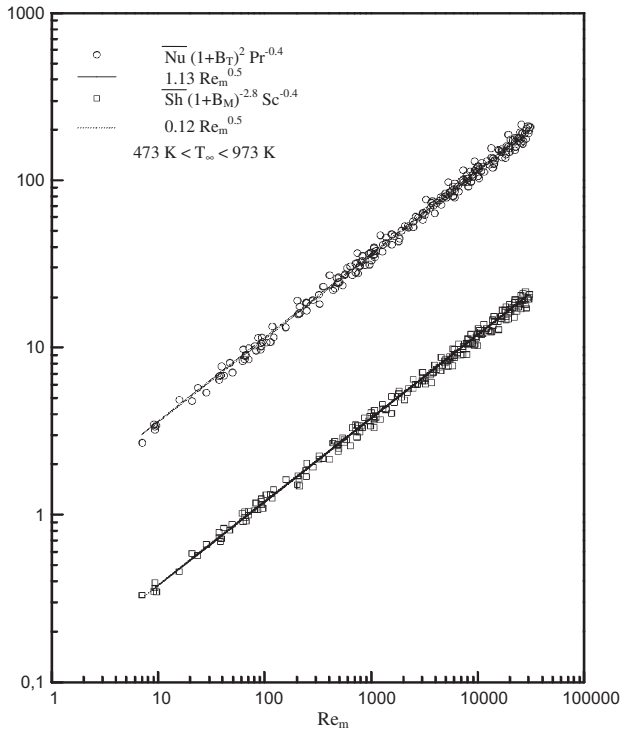

Fig. 13. Mean Nusselt and Sherwood numbers correlations as function of thermal and mass transfer numbers.

5. Conclusion

A numerical analysis of heat and mass transfer around rotating hexane liquid droplet, assumed as a hard sphere, is developed. Heat and mass transfer equations are solved using an implicit finite difference scheme taking into account the variability of thermophysical and transport properties.

A comparison of the mean Nusselt number and that of Kreith shows a good agreement for monocomponent hydrocarbons. This phenomenon determines, at first, a similar correlation of Sherwood number for pure hydrocarbons by taking into account the effect of the evaporation. Further, the evaporation of the rotating sphere, hexane saturated liquid, is considered by analyzing the influence of the rotation on physical parameters and the growth of the vapour phase thickness. It is observed that there exists two kinds of forces, the buoyancy and the repulsion forces. These forces are due to the centrifugal forces which generate a thermal plume on the top of the liquid droplet and move away quickly the released vapour from the droplet surface to a location where the rotation is weak.

Secondly, correlations expressing the mean Nusselt and Sherwood numbers as a function of Reynolds, Prandtl, Schmidt, heat and mass transfer numbers, are proposed. These correlations taken into account the effect of the evaporation phenomena and the heat and mass transfer in the vapour phase surrounding the rotating liquid droplet.

Aknowledgement

This work has been Granted by the Lebanese CNRS under contract number 2225.

Appendix A

The algorithm of resolution of the mathematical model can be described by the following instructions:

1. Initialization of the physical parameters and properties (temperature, velocities, concentration,. . ..).
2. Determination of the thermophysical and transport properties and solution of the energy equation, the mass diffusion equation, the Navier–Stokes equations and the continuity equation by using the boundary conditions (4)–(9).
3. Test on the vapour phase temperature: if the test is greater than a specific value of 10^{-3}, the program increases the thickness of the boundary layer and returns to stage 2.
4. Determination of local Nusselt and Sherwood numbers.

5. Test on the angle: if the (θ) angle is lower than 180°, local Nusselt and Sherwood numbers have been determined and the step ($\Delta\theta$) has been increased of one value before returning to stage 2. If this angle is greater than this same value, the program of the calculus stops.
6. Computation of average Nusselt and Sherwood numbers by Simpson integration.

References

[1] C. Chauveau, X. Chesneau, I. Gökalp, Paper presented at the 31th Aerospace Sciences Meeting, Reno, AIAA (1993) 11–14.
[2] J.P. Deplanque, W.A. Sirignano, Numerical study of the transient vaporization of an oxygen droplet at sub and super critical conditions, Int. J. Heat Mass Transfer 36 (1993) 4419–4431.
[3] M. Bouaziz, A. Daïf, A. Ali Chérif, X. Chesneau, Paper Presented at the International Symposium in Computational Heat Transfer, Turkey, Cesme, 1997 pp. 222–224.
[4] B. Gebhart, C.A. Hieber, Mixed convection from a sphere at small Reynolds and Grashof numbers, J. Fluid Mech. 38 (1969) 137–159.
[5] T. Yuge, Experiments on heat transfer from spheres including natural and forced convection, J. Heat Transfer 82 (1960) 214–220.
[6] W.S. Amato, C. Tien, Free convection heat transfer from isothermal spheres in water, Int. J. Heat Mass Transfer 15 (1972) 327–339.
[7] W.E. Ranz, W.R. Marshall, Evaporation from drops, Chem. Eng. Prog. 48 (1952) 141–173.
[8] T.S. Chen, A. Mucoglu, Analysis of mixed forced and free convection around a sphere, Int. J. Heat Mass Transfer 20 (1993) 867–875.
[9] M. Renksizbulut, M.C. Yuen, Numerical study of droplet evaporation in a high temperature stream, J. Heat Transfer 105 (1983) 389–397.
[10] J. Dgheim, X. Chesneau, L. Pietri, B. Zeghmati, Heat and mass transfer correlations for liquid droplet of a pure fuel in combustion, Heat Mass Transfer 38 (2002) 543–550.
[11] S.S. Sazhin, Advanced models of fuel droplet heating and evaporation, Prog. Energy Combust. Sci. 32 (2006) 162–214.
[12] F. Kreith, L.G. Roberts, J.A. Sullivan, S.N. Sinha, Convection heat transfer and flow phenomena of rotating spheres, Int. J. Heat Mass Transfer 6 (1963) 881–895.
[13] P. Saikrishnan, S. Roy, Steady nonsimilar axisymmetric water boundary layers with variable viscosity and Prandtl number, Acta Mech. 157 (2002) 187–199.
[14] P. Saikrishnan, S. Roy, Non uniform slot injection (suction) into steady laminar water boundary layer flow over a rotating sphere, Int. J. Heat Mass Transfer 46 (2003) 3389–3396.
[15] S.J. Garrett, N. Peake, The stability and transition of the boundary layer on a rotating sphere, J. Fluid Mech. 456 (2002) 199–218.
[16] E.K.W. Poon, A.S.H. Ooi, M. Giacobello, R.C.Z. Cohen, Laminar flow structures from a rotating sphere: effect of rotating axis angle, Int. J. Heat Fluid Flow 31 (5) (2010) 961–972.
[17] J. Dgheim, Contribution study of the evaporation and the combustion of liquid hydrocarbons droplets, PhD Thesis, University of Perpignan, France 2001.
[18] A. Lieberam, VDI, Verlag GmbH, Dusseldorf, Leverkusen, December 1 to December 38, 1993.
[19] B. Abramzon, W.A. Sirignano, Paper presented at the Proceeding of Thermal Engineering, Joint Conference, Honolulu, ASME6JSME, 1987 pp. 11–18.